

## Supplementary Information

### Profiling drugs for rheumatoid arthritis that inhibit synovial fibroblast activation

Douglas S. Jones<sup>1,2</sup>, Annie P. Jenney<sup>1</sup>, Jennifer L. Swantek<sup>3</sup>, John M. Burke<sup>3,4,5</sup>, Douglas A. Lauffenburger<sup>2</sup>, Peter K. Sorger<sup>1\*</sup>

<sup>1</sup> HMS LINCS Center, Laboratory of Systems Pharmacology, Harvard Medical School, Boston, MA 02115

<sup>2</sup> Department of Biological Engineering, Massachusetts Institute of Technology, Cambridge, MA, 02139

<sup>3</sup> Immunology and Inflammation, Boehringer Ingelheim, Ridgefield, CT 06877

<sup>4</sup> Systems Biology, Boehringer Ingelheim, RidgeField, CT 06877

<sup>5</sup> Present address: Applied BioMath LLC, Winchester, MA 01890

\*Address correspondence to:

Peter K. Sorger

WAB Room 438, Harvard Medical School, 200 Longwood Avenue, Boston MA 02115

Tel: 617-432-6901

Email: peter\_sorger@hms.harvard.edu, cc: Christopher\_Bird@hms.harvard.edu

## Supplementary Results

**Supplementary Table 1.** List of abbreviations

Abbreviation	Name
5ZO	(5z)-7-oxozeaenol
6CK	6 cytokine set (comprising IL-6, IL-8, RANTES, IP-10, MCP-1, GRO $\alpha$ )
AKT	Also protein kinase B (PKB)
EGF	Epidermal growth factor
ERK	Extracellular-signal-regulated kinase
FGF Basic	Fibroblast growth factor basic (also FGF-2)
G-CSF	Granulocyte-colony stimulating factor
GRO $\alpha$	Growth regulated oncogene $\alpha$ (also CXCL1)
IGF	Insulin-like growth factor
IKK	I $\kappa$ B kinase
IL-16	Interleukin 16
IL-17	Interleukin 17
IL-1 $\alpha$	Interleukin 1 $\alpha$
IL-6	Interleukin 6
IL-8	Interleukin 8
iMLR	MLR with interaction terms
IP-10	Interferon gamma-induced protein 10 (also CXCL10)
JAK	Janus kinase
JNK	Jun N-terminal kinase
MAP2K	Mitogen activated protein kinase kinase (also MAPKK, MAPK kinase)
MAP3K	Mitogen activated protein kinase kinase kinase (also MAPKKK, MAP2K kinase)
MAPK	Mitogen activated protein kinase
MCP-1	Monocyte chemotactic protein 1 (also CCL2)
MCP-3	Monocyte chemotactic protein 3 (also CCL7)
MEK	Mitogen activated protein kinase (MAPK) ERK kinase (also MAPK kinase, MAP2K)
MIG	Monokine induced by gamma interferon (also CXCL9)
MKK6	Mitogen activated protein kinase (MAPK) kinase 6 (also MAPKK 6, MAP2K6)
MLR	Multiple linear regression
NF $\kappa$ B	Nuclear factor- $\kappa$ B
ns	No stimulus
P38	P38 mitogen activated protein kinase
PI3K	Phosphatidylinositol-3-kinase
Poly(I:C)	Polyinosinic:polycytidylic acid
RA	Rheumatoid arthritis
RANTES	Regulated on activation, normal T cell expressed and secreted (also CCL5)
SF	Synovial fibroblasts
STAT	Signal transducer and activator of transcription
TAK1	TGF- $\beta$ activated kinase 1 (also MAPK kinase kinase 7, MAP3K7)
TNF $\alpha$	Tumor necrosis factor $\alpha$

**Supplementary Table 2.** Synovial fibroblast donor samples\*

Sample	Company Lot. No.	Disease Type
N2586	2586	Normal
N2645	2645	Normal
N2759	2759	Normal
RA1869	1869	RA
RA1931	1931	RA
RA2159	2159	RA
RA2708	2708	RA

\*Synovial fibroblasts were purchased from Cell Applications, Inc. “Disease type” normal are human fibroblast like synoviocytes (HFLS) cat. no. 408–05a, and disease type RA are HFLS–RA (cat. no. 408RA–05a).

**Supplementary Table 3.** Information about stimuli

Type	Name	Relationship to RA or SF biology
Inflammatory cytokines	TNF $\alpha$ (tumor necrosis factor $\alpha$ )	TNF neutralizing biologics etanercept (Enbrel®), infliximab (Remicade®), and adalimumab (Humira®) are front–line therapy following disease modifying anti–rheumatic agents (DMARDs) <sup>1,2</sup>
	IL–1 $\alpha$ (interleukin 1 $\alpha$ )	FDA approved biologic anakinra (Kineret®) is a recombinant IL–1 receptor antagonist <sup>2</sup>
	IL–6 (interleukin 6)	FDA approved biologic tocilizumab (Actemra®) inhibits the interaction of IL–6 with the IL–6 receptor <sup>2</sup>
	IL–17 (interleukin 17)	Induces IL–6 and IL–8 secretion in synovial fibroblasts <sup>3</sup>
Adipokines	Adiponectin	Adipose–derived cytokine with potential role in inflammation and immunity <sup>4,5</sup>
	Visfatin	Adipose–derived cytokine with potential role in inflammation and immunity <sup>4,5</sup>
	Leptin	Adipose–derived cytokine with potential role in inflammation and immunity <sup>4,5</sup>
Growth factors	EGF (epidermal growth factor)	Elevated levels in RA and active towards SF <sup>6</sup>
	IGF (insulin–like growth factor)	Elevated levels in RA and levels inversely correlated with systemic inflammation <sup>7,8</sup>
Toll–like receptor (TLR) agonist	Poly(I:C) (polyinosinic:polycytidylic acid)	TLR3 agonist, mimics viral infection, which is a cause of RA flare–ups <sup>9</sup>

**Supplementary Table 4.** Information about stimulatory factors and signature cytokine set

<b>Abbreviation</b>	<b>Name</b>	<b>Alternative names</b>	<b>Function</b>
IL-6	Interleukin 6	n/a	Neutrophil and T lymphocyte chemoattractant, T and B cell differentiation <sup>10</sup>
IL-8	Interleukin 8	CXCL8 ((c-x-c motif) ligand 8)	Neutrophil chemoattractant <sup>11</sup>
GRO $\alpha$		CXCL1 ((c-x-c motif) ligand 1)	Neutrophil chemoattractant <sup>12,13</sup>
MCP-1	Monocyte chemotactic protein 1	CCL2 (c-c motif) ligand 2	Monocyte, T cell, and dendritic cell chemoattractant <sup>14,15</sup>
RANTES	Regulated on activation, normal T cell expressed and secreted	CCL5 (c-c motif) ligand 5	Natural killer cell mitogen <sup>16</sup> , leukocyte chemoattractant <sup>17</sup>
IP-10	Interferon $\gamma$ -induced protein 10	CXCL10 (c-x-c motif) ligand 10	Monocyte and T lymphocyte chemoattractant <sup>18</sup>

**Supplementary Table 5.** Synovial fluid samples\*

<b>Sample</b>	<b>Company Lot. No.</b>	<b>Disease Type</b>
Synovial fluid A	1112050075	RA
Synovial fluid B	118050105	RA
Synovial fluid C	111050045	RA
Synovial fluid D	113060040	RA

\*Synovial fluids were purchased from Analytical Biological Services, Inc.

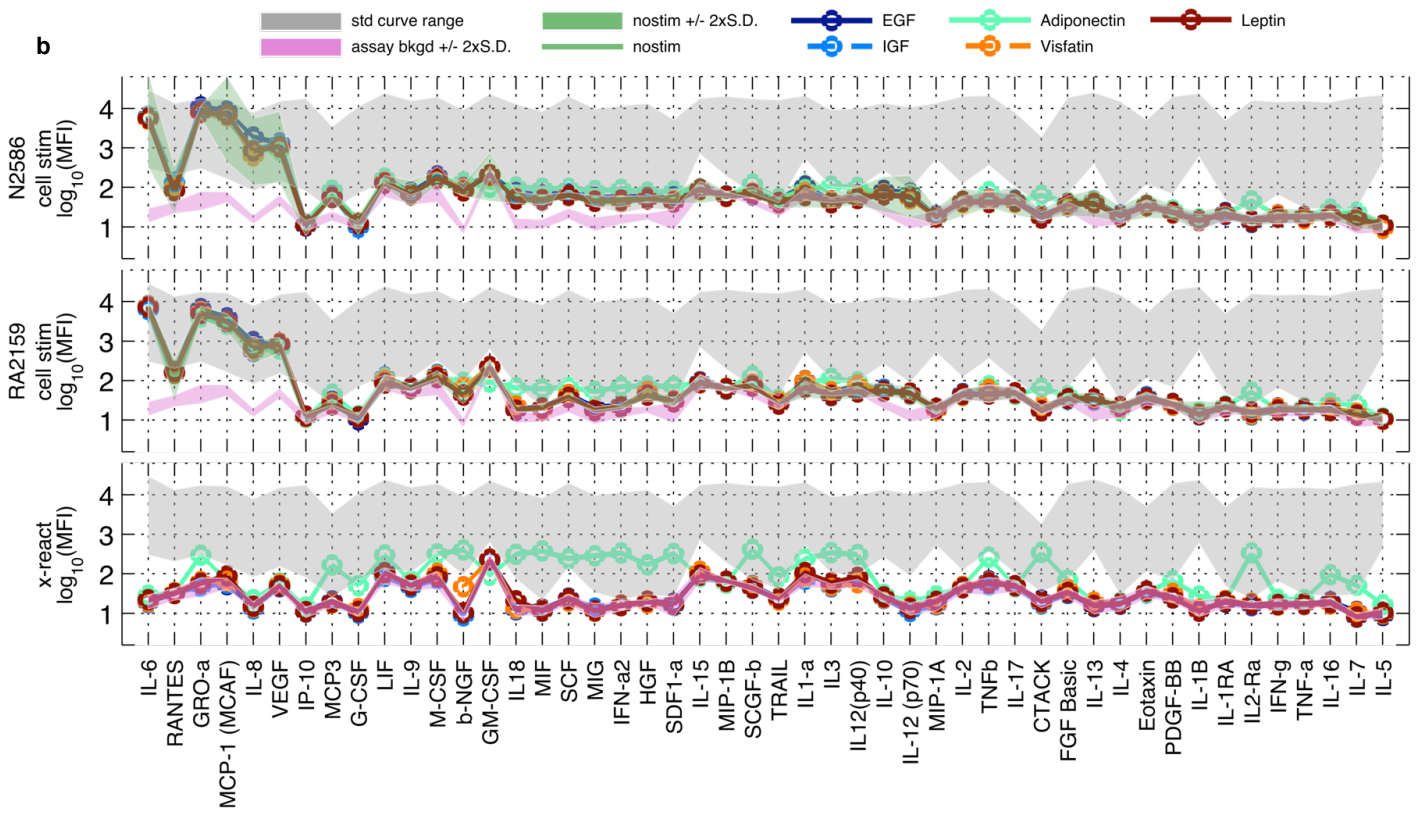
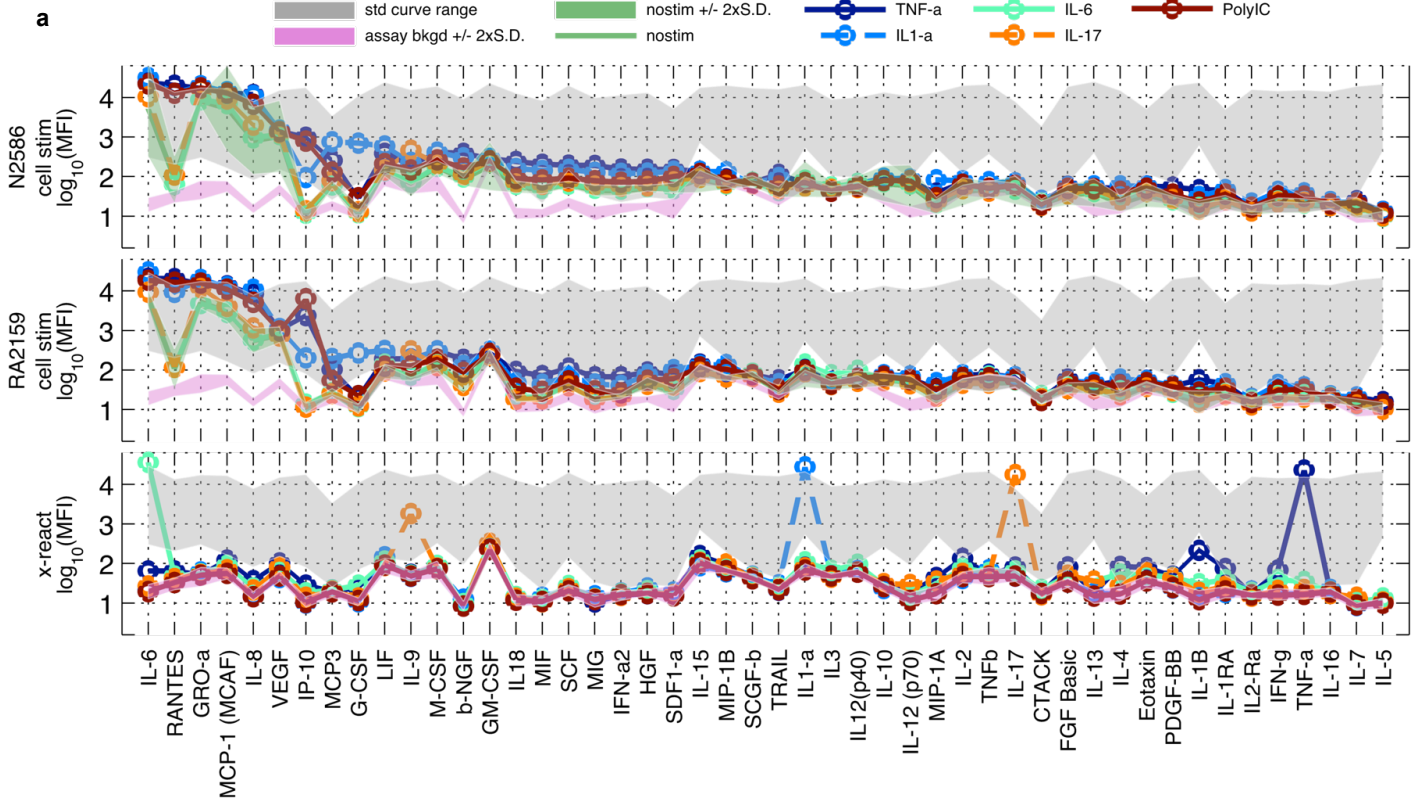
**Supplementary Table 6.** Information small molecule inhibitors used in this study. All attempts were made to use inhibitors with high specificity to its primary target.

Pathway	Name	Supplier	Target	Secondary target (if known)
MEK/ERK	CI-1040 (PD184352)	Selleck (cat. no. S1020)	MEK1/2 <sup>19</sup>	Good specificity <sup>19,20</sup> (allosteric)
	PD0325901	Selleck (ca. no. S1036)	MEK1/2 <sup>21</sup>	Good specificity (allosteric)
PI3K/AKT	GDC-0941	Haoyuan Chemexpress (HY-10358)	PI3K <sup>22</sup>	Good specificity <sup>20</sup>
	MK2206	Haoyuan Chemexpress (HY-50094)	AKT <sup>23</sup>	Good specificity (allosteric) <sup>23</sup>
P38	SB202190	Selleck (cat. no. S1077)	P38 <sup>19</sup>	Good specificity <sup>19</sup>
	PH-797804	Selleck (cat. no. S2726)	P38 <sup>24</sup>	Good specificity <sup>24</sup>
JAK/STAT	Tofacitinib (Xeljanz®, CP-690550)	Selleck (cat. no. S2789)	JAK3 <sup>25</sup>	JAK1/2 <sup>25</sup>
	Ruxolitinib (Jakavi®, INCB018424)	Selleck (cat. no. S1378)	JAK1/2 <sup>26</sup>	TYK2 <sup>26</sup>
	Lestaurtinib (CEP- 701)	LC Labs (cat. no. L- 6307)	JAK2 <sup>27</sup>	FLT3 <sup>28</sup> , TrkA <sup>29</sup> , others <sup>20</sup>
JNK	JNK-IN-8	Nathanael Gray (Dana Farber Cancer Institute)	JNK1/2/3 <sup>30</sup>	Good specificity <sup>30</sup>
IKK/NFκB	IKK 16	Tocris (cat. no. 2539)	IKK-1/2 <sup>31</sup>	JNK, JAK (Supplementary Fig. 5)
TAK1	(5z)-7-oxozeanol	Tocris (cat. no. 3604)	TAK1	MEK1/2 <sup>32</sup>
	NG25	ChemScene CS-0875	TAK1	MAP4K2 <sup>33</sup>

**Supplementary Table 7.** MLR solution algorithms

Algorithm Type	Method	Method Subset
No stepwise	p-value tests	With multiple hypothesis correction (FDR- controlled)
		Without multiple hypothesis correction
Stepwise regression	p-value tests	Forward addition (FDR-controlled)
		Backward elimination (FDR-controlled)
		AIC
		Corrected AIC (AICc)
	BIC	Forward addition
		Backward elimination

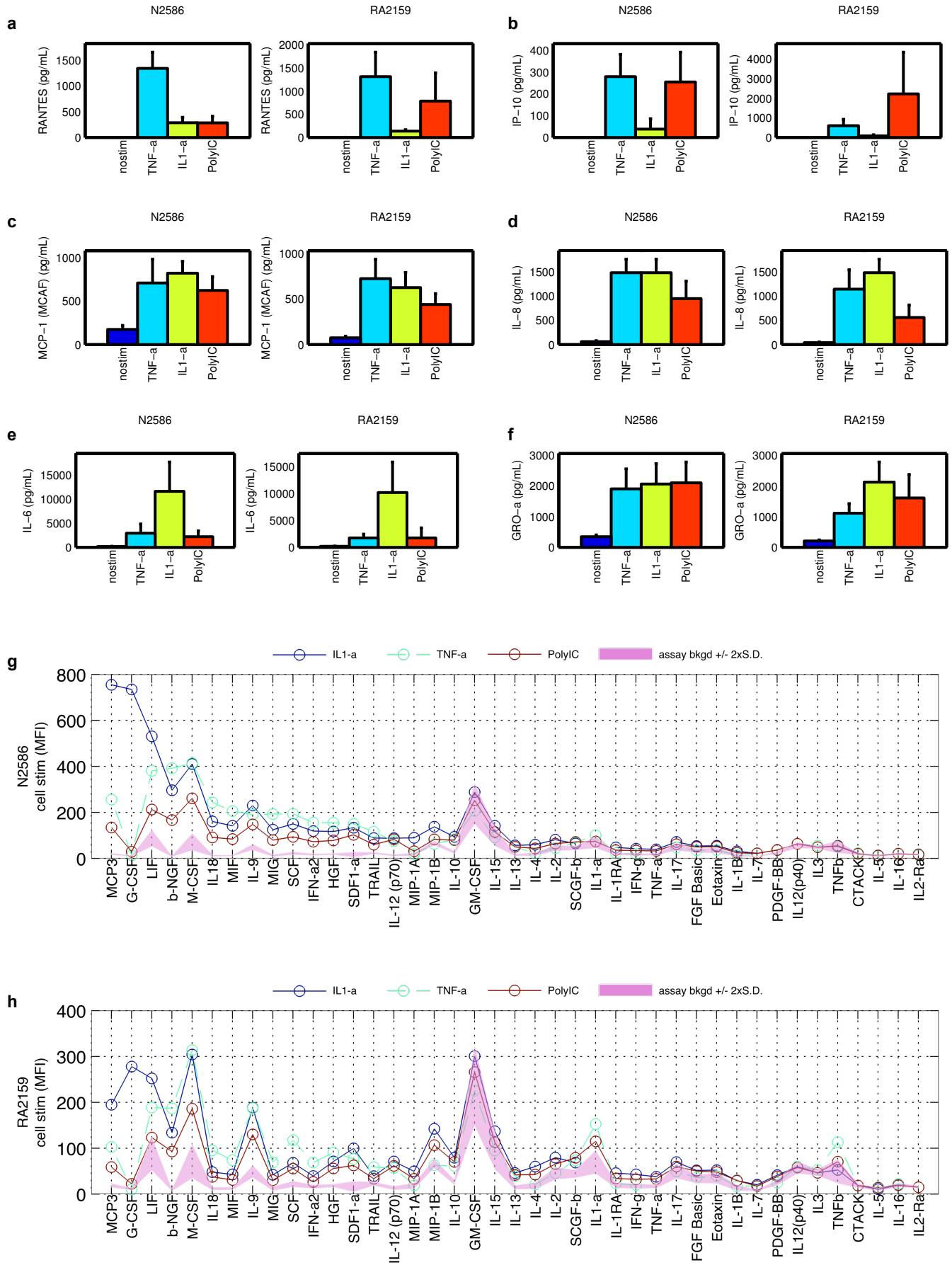
# Supplemental Figure 1



**Supplementary Figure 1 Cytokine profiling of primary human SF from one normal (N2586) and one RA (RA2159) donor following individual stimulation with 1 of 10 stimuli** (from

Dataset 1, related to Fig. 1d). **(a–b)** Secretion response of SF samples N2586 (top plot of each panel) or RA2159 (middle plot of each panel) the 10 stimuli (panel **a**: TNF $\alpha$ , IL-1 $\alpha$ , IL-6, IL-17, or Poly(I:C); panel **b**: EGF, IGF, adiponectin, visfatin, or leptin). The 10 stimuli were split into two panels for easier visualization; TNF $\alpha$ , IL-1 $\alpha$ , and Poly(I:C) are replotted from Fig. 1. Assay background ( $\pm 2$  standard deviations (S.D.) from the mean) is shown in purple, upper and lower boundaries for each cytokine (dynamic range; derived from the standard curve for each measured cytokine) is shown in gray, and basal secretion levels ( $\pm 2$  S.D.) are shown in green. Cross-reactive signal of the stimuli against luminex analytes is shown on the bottom plot of each panel. For top and middle panels, conditions where the stimulus is the same as the measured species have been filtered to not-a-number (NaN), e.g. measurement of TNF $\alpha$  supernatant levels following stimulation of TNF $\alpha$  has been filtered to NaN, and are excluded from the analysis. TNF $\alpha$ , IL-1 $\alpha$ , and Poly(I:C) strongly induce secretion of the 6CK set (IL-6, RANTES, GRO $\alpha$ , MCP-1, and IL-8) in both the normal and RA SF samples, while stimulation with IL-6 and IL-17, for example, largely tracks the basal secreted levels (green shaded region).

# Supplemental Figure 2

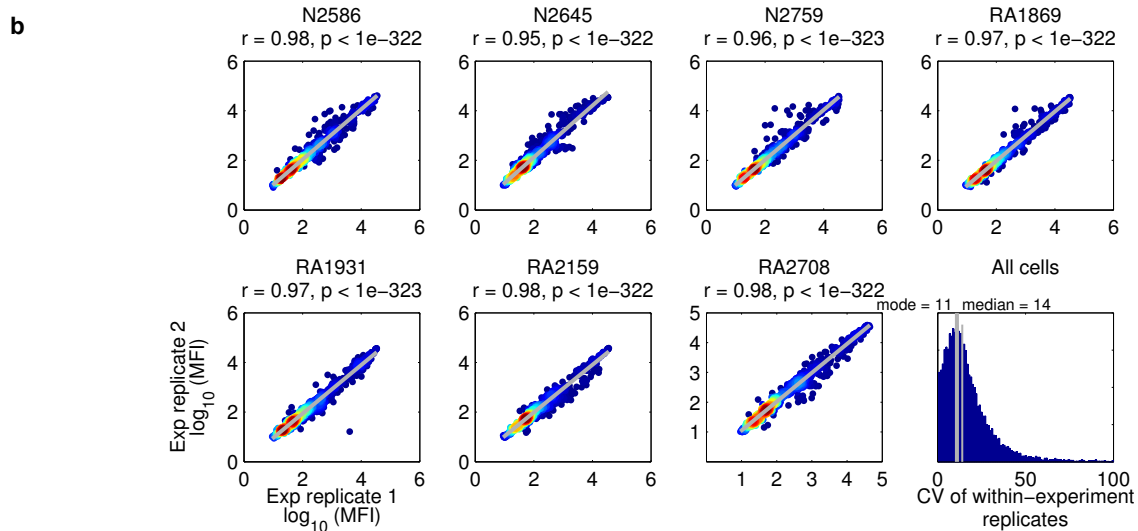
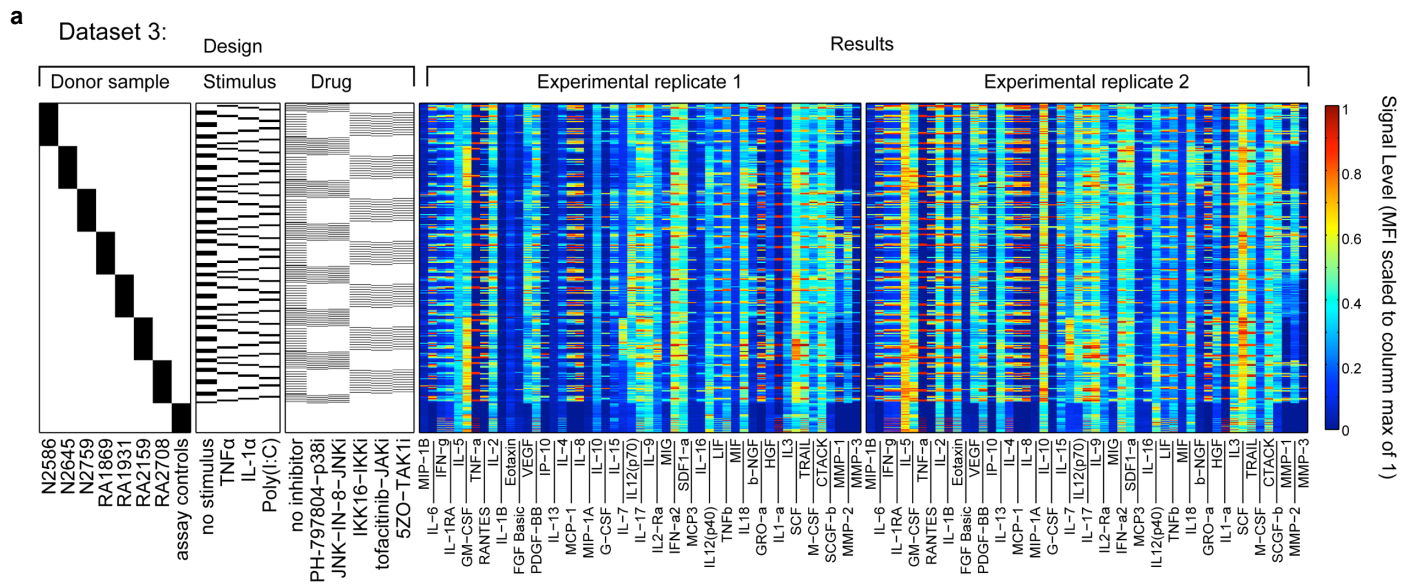


**Supplementary Figure 2** *Secretion of 6CK set cytokines and filtered cytokine profiles of non-6CK set cytokines* (from Dataset 1). **(a–f)** Secretion of 6CK set cytokines (IL–6, IL–8, RANTES, IP–10, GRO $\alpha$ , and MCP–1) from one normal (N2586) and one RA (RA2159) SF samples following stimulation with TNF $\alpha$ , IL–1 $\alpha$ , or Poly(I:C). Each of these cytokines is induced to at least 500 pg/mL in one or more of the conditions examined. **(g–h)** Filtered secretion response measurements for SF samples N2586 (panel **g**) and RA2159 (panel **h**). MFI values were filtered by subtracting basal secretion levels and cross–reactivity by stimulating–ligands against kit components. Following this filtering several factors remain detectable above the assay baseline.



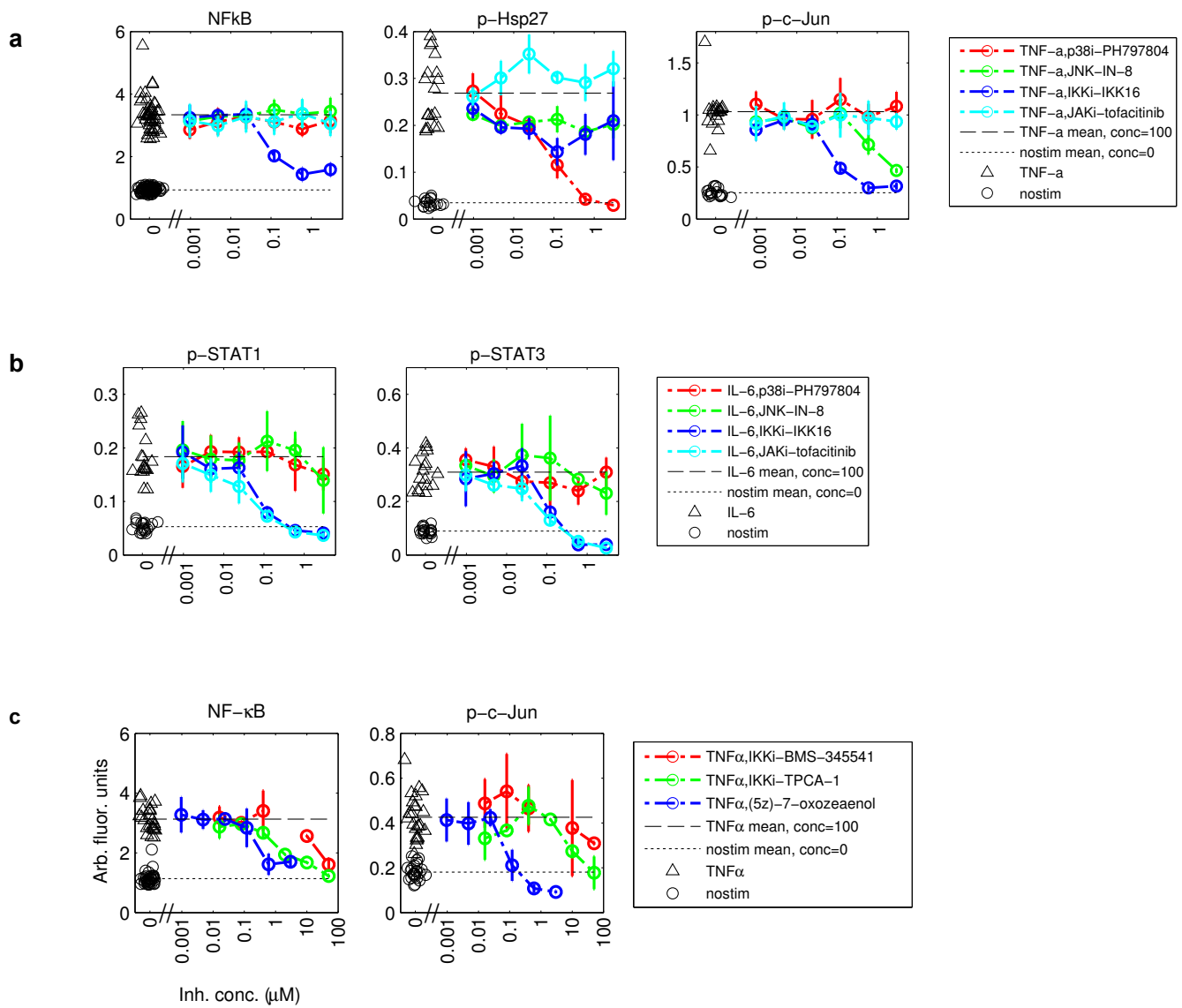
**Supplementary Figure 3** *Correlational analysis of cytokine profiles from SF supernatants and RA synovial fluid.* (a) Pearson correlation of cytokine profiles from SF donor samples N2586 and RA2159 reveals a weak positive correlation between basal secretion and RA synovial fluid composition; this positive correlation is largely unchanged for many of the stimuli. However, an apparent increase in correlation is observed for TNF $\alpha$  and Poly(I:C). (b) The partial Pearson correlation between SF supernatants and RA synovial fluids, when controlling for the variance explained by basal secretion identifies TNF $\alpha$ , IL-1 $\alpha$ , and Poly(I:C) as inducing a cytokine secretion response in SF that is significantly correlated to the profiles of RA synovial fluids (panel **b** bottom). Binned values for the false discovery rate (FDR) corrected p-values were assigned positive or negative values according to the sign of the partial correlation. Euclidean distances between basal and induced supernatant cytokine profiles provide a univariate metric for the magnitude of the secretion response induced by each stimulus (panel **b** top); the factors inducing the strongest secretion response in the N2586 and RA2159 SF samples (TNF $\alpha$ , IL-1 $\alpha$ , and Poly(I:C), top) are doing so in a manner that is significantly correlated to the composition of the three RA synovial fluids (bottom). False discovery rate (FDR) controlled by Benjamini–Hochberg method.<sup>34</sup>

# Supplemental Figure 4



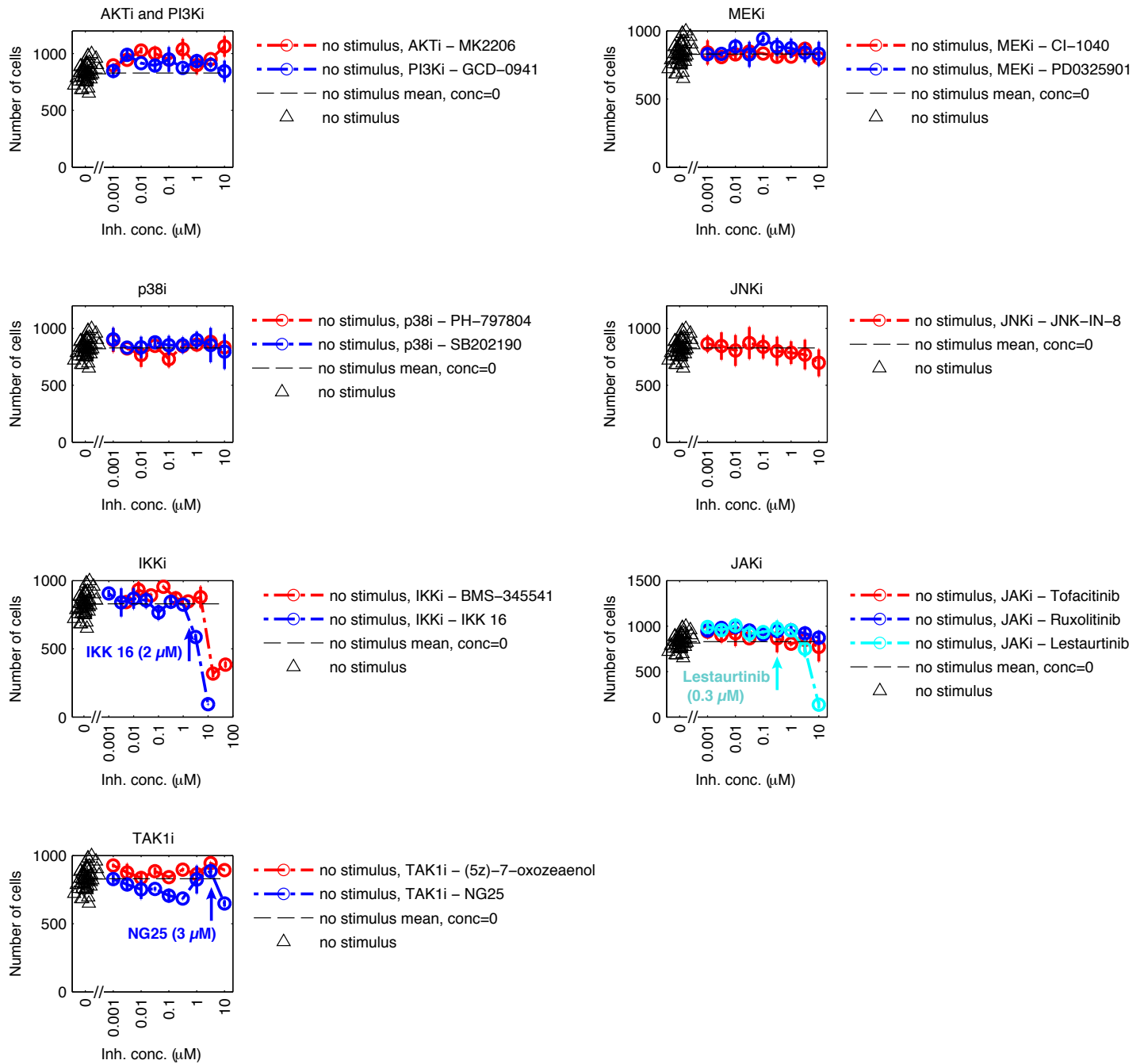
**Supplementary Figure 4 *Strong consistency between independent experimental replicates of Dataset 3.*** (a) Experimental design (left) and results (right) for Dataset 3. Black shading denotes the inclusion in an experiment of one of seven donor samples, one of three cytokines (TNF $\alpha$ , IL-1 $\alpha$ , or Poly(I:C)) and one of five inhibitors. The measured levels of the 51 cytokines and proteases in cell supernatants are shown as raw median fluorescent intensity scaled column-wise to a maximum of 1 and displayed as a heat map; each row represents one sample. A full experimental replicate was performed on a separate day (replicates 1 and 2). (b) The two experimental replicates show a strong Pearson correlation ( $r > 0.95$ ). Coefficient of variation (CV) of biological replicates within the same experiment is low (median=14% CV) and follows a Gaussian distribution (bottom right).

# Supplemental Figure 5



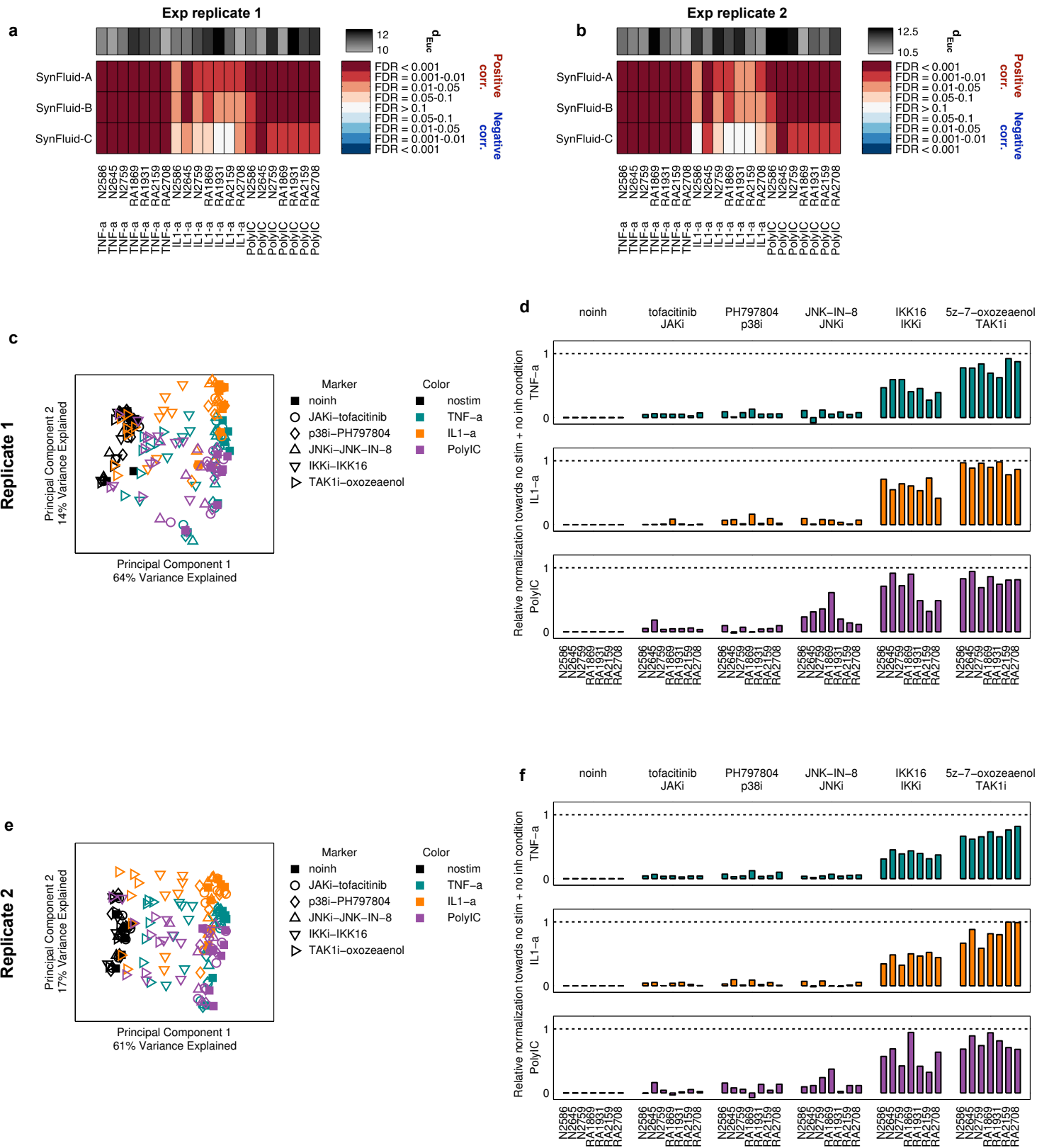
**Supplementary Figure 5 Activity and specificity of p38, JNK, IKK, and JAK inhibitors used in Dataset 3.** The inhibitors were evaluated based on their inhibition of the NFκB pathway (via NFκB nuclear translocation), p38 pathway (via Hsp27 phosphorylation), and JNK pathway (via c-Jun phosphorylation) following 30 min stimulation with 100 ng/mL TNFα (panel **a**) or inhibition of the JAK pathway (via STAT1 and STAT3 phosphorylation) following 30 min stimulation with 100 ng/mL IL-6 (panel **b**). The p38 inhibitor (PH-797804), JNK inhibitor (JNK-IN-8), and JAK inhibitor (tofacitinib) each exhibited strong specificity, potently inhibiting the respective on-target pathway, with minimal off-target effects. IKK 16 inhibited TNFα-induced NFκB in a dose-dependent manner, but also displayed polypharmacology against TNFα-induced p-cJun and IL-6-induced p-STAT1 and p-STAT3, which are not believed to be activated by the IKK/NFκB pathway. (c) Two other inhibitors considered to be specific for IKK displayed weak potency towards NFκB signaling and also displayed polypharmacology towards JNK. The more specific of these two inhibitors (BMS-345541) was toxic at 10 μM (see Supplementary Fig. 16), even though its IC90 was ~50 μM. For these reasons IKK 16 was selected for use in Dataset 3.

# Supplemental Figure 6

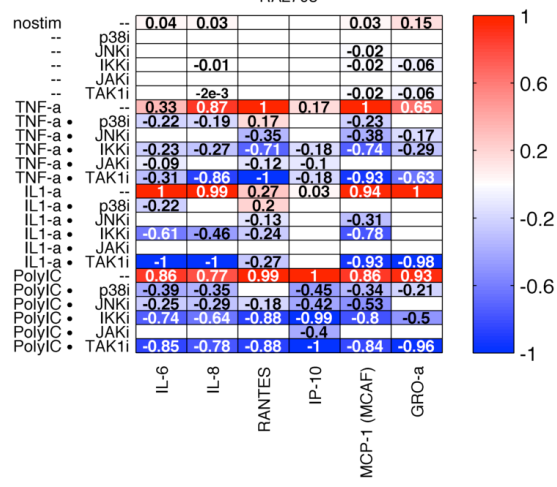
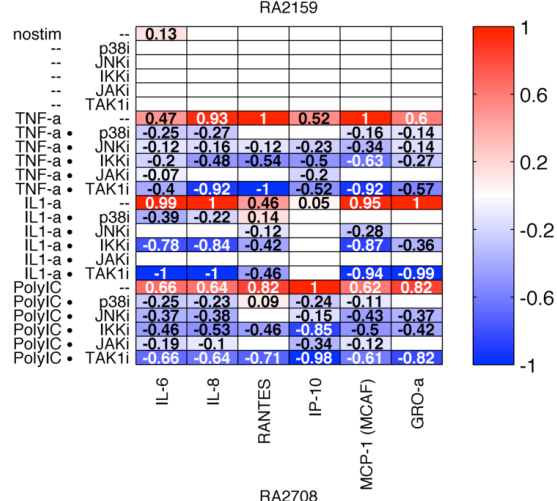
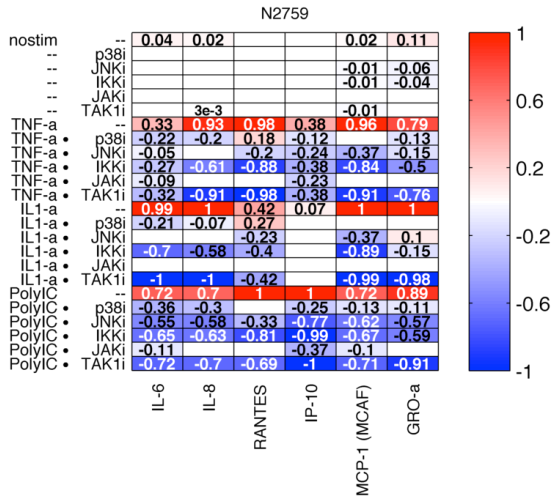
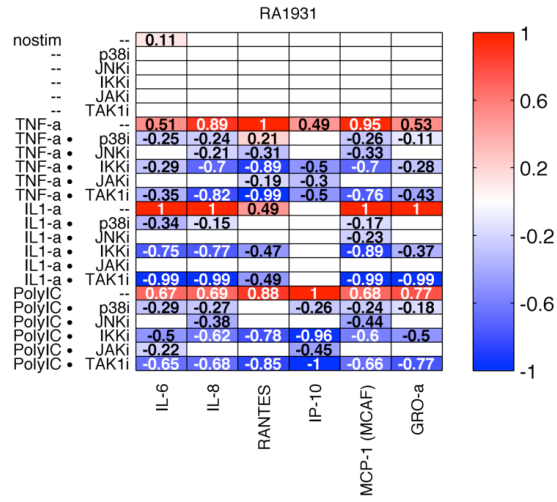
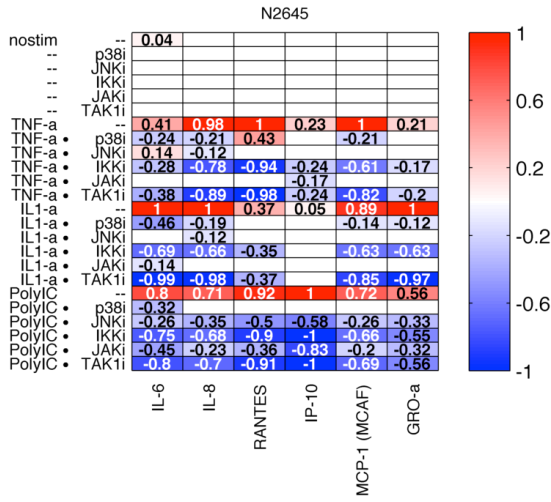
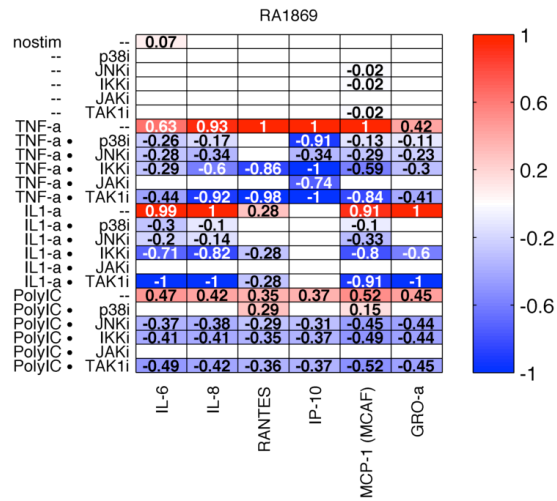
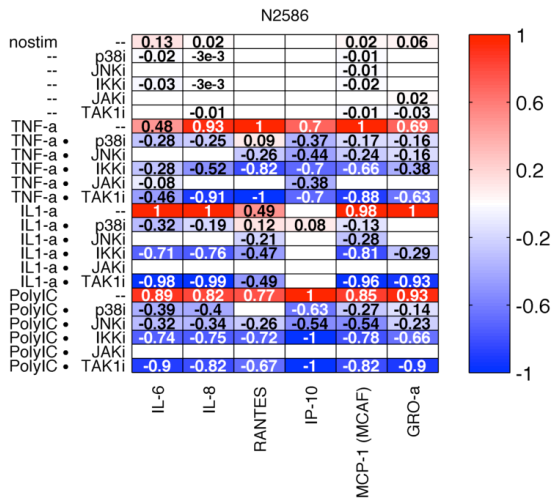


**Supplementary Figure 6** *Toxicity profiling of kinase inhibitors on SF.* Cell counts (by high-throughput microscopy) following 24 hr exposure of SF in serum free medium to serial dilutions of kinase inhibitors confirms that inhibitors used in this study were used below toxic doses. For inhibitors used in this study that show toxicity in the range of this assay we have indicated the concentration used in cytokine secretion assays with an arrow.

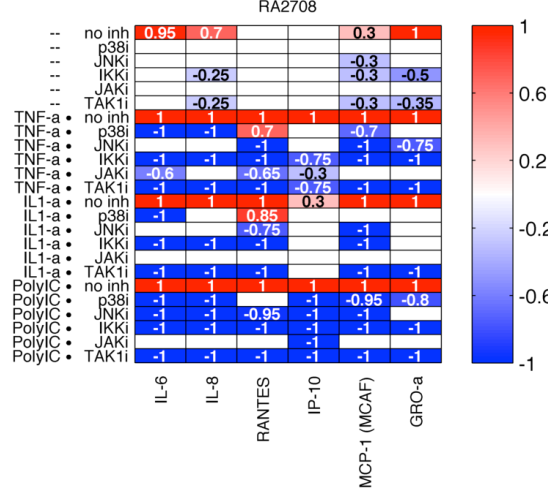
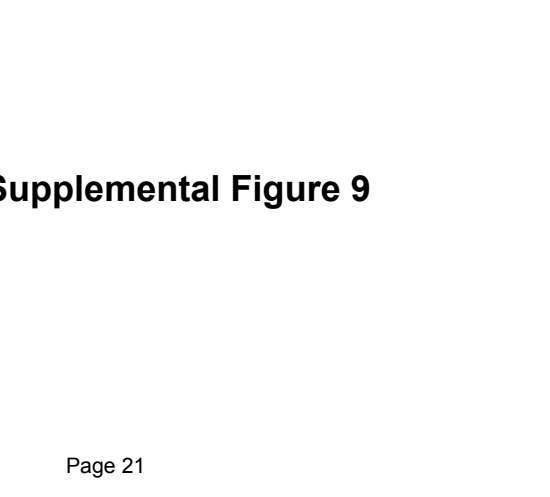
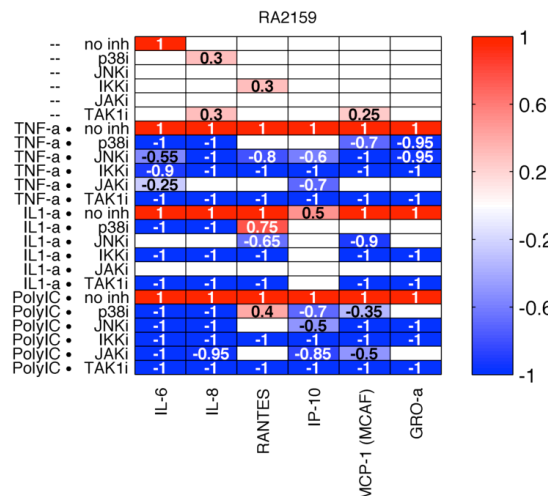
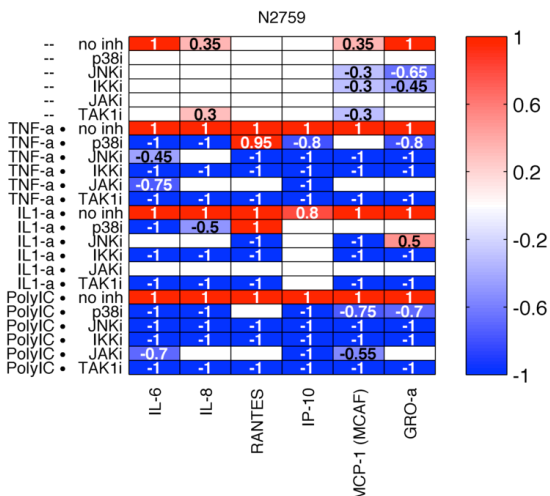
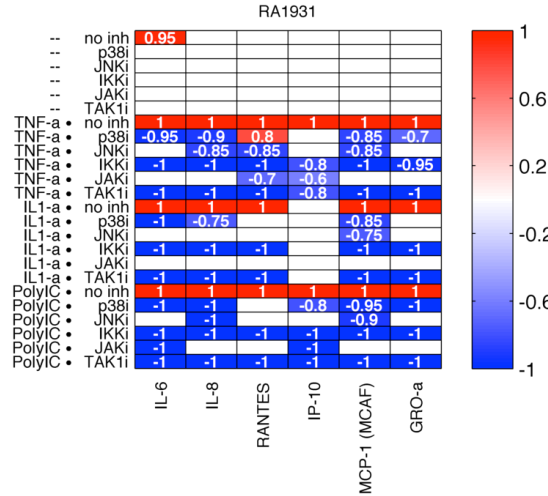
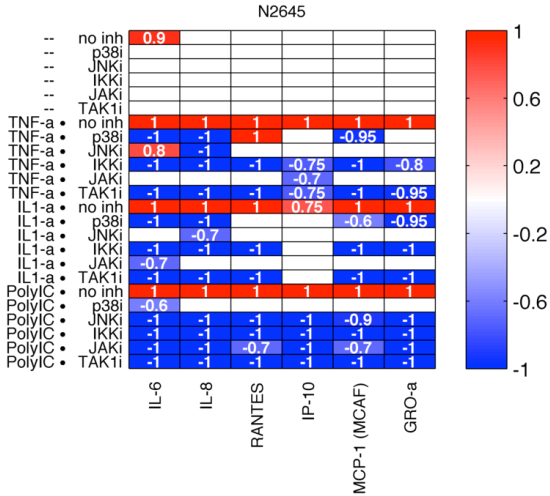
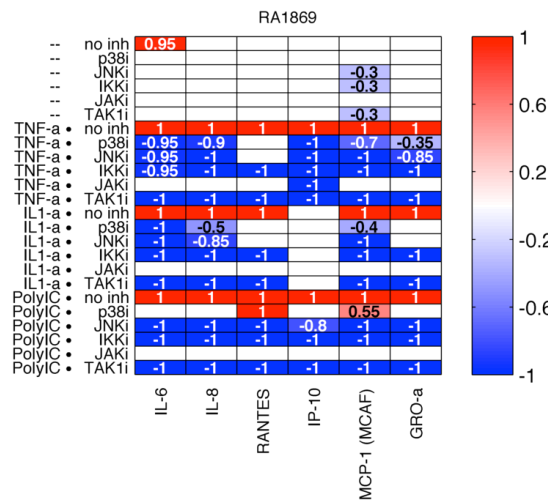
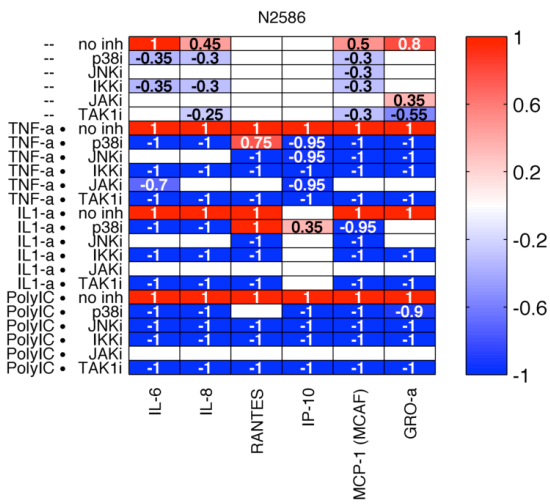
# Supplemental Figure 7



**Supplementary Figure 7 Comparison of activated SF cytokine profiles and RA synovial fluid profiles and multivariate analysis of inhibitor effects.** (a–b) TNF $\alpha$ , IL–1 $\alpha$ , and Poly(I:C) each induce strong secretion response across the three normal and four RA SF samples (top; gray–scale heat maps) in both experimental replicate 1 (panel a) and 2 (panel b) as quantified by the Euclidean distance of the secretion response profile from basal secretion levels for each SF donor sample. Secretion profiles of SF activated by TNF $\alpha$ , IL–1 $\alpha$ , and Poly(I:C) each have a significant partial Pearson correlation to cytokine profiles from three independent RA synovial fluids (when controlling for variance explained by the basal secretion levels of each individual SF donor sample; (bottom; red heat maps). False discovery rate controlled by Benjamini–Hochberg method<sup>34</sup>. (c–f) Evaluation of inhibitor effects on activated SF cytokine profiles using PCA for experimental replicates 1 (panels c–d) and 2 (panels e–f). Principal component 1 (PC 1) distinguishes secretion response landscapes of basal vs. stimulated cells, while PC 2 distinguishes stimulatory context (panels c,e). Donor–to–donor variability results in scatter along PC2. A univariate metric for inhibitor effects on the multivariate secretion profile can be computed by considering the location of the stimulus+inhibitor condition with respect to the basal and uninhibited stimulus conditions in PC space as described for Fig. 2 (panels d,f). A value of 0 indicates no effect of the inhibitor and a value of 1 complete normalization to basal levels.



Supplemental Figure 8



Supplemental Figure 9





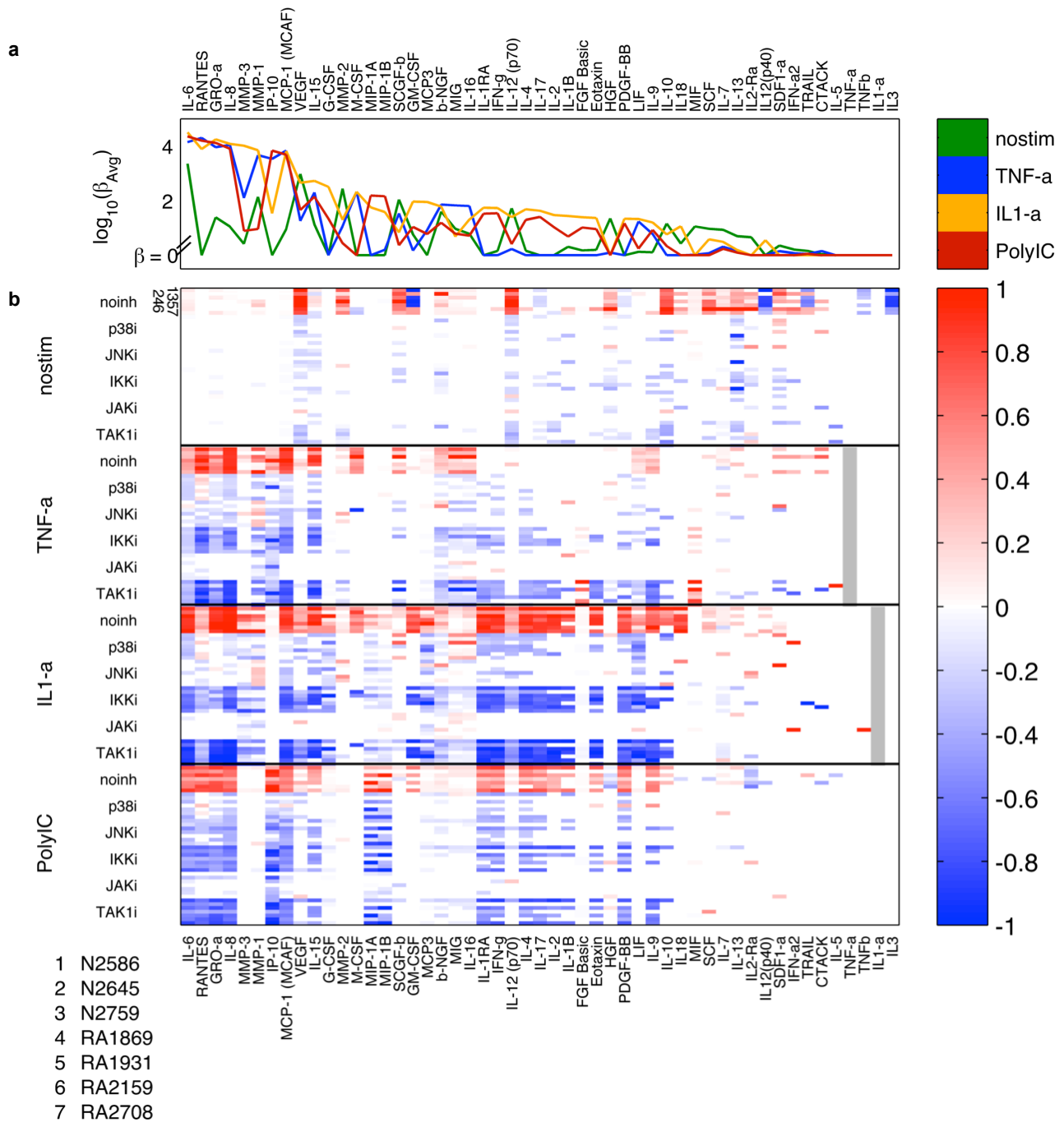
**Supplementary Figure 8  $\beta$  coefficients for stimuli, inhibitor, and context-dependent inhibitor effects for the 6CK set calculated from Dataset 3** (related to Fig. 3d). Coefficients were merged across the two experimental replicates of Dataset 3 and scaled to a maximum of 1 for each column. SF sample N2586 is reproduced from Fig. 3d for ease of comparison.

**Supplementary Figure 9 Confidence weights of  $\beta$  coefficients for the 6CK set**; representing the fraction out of the 10 multimodeling approaches (outlined in Supplementary Table 7) that assign a significant effect to the given  $\beta$  coefficient (related to Fig. 3d and Supplementary Fig. 8). Confidence weights for  $\beta$  coefficients were merged across the two experimental replicates of Dataset 3.

**Supplementary Figure 10  $\beta$  coefficients for stimuli, inhibitor, and context-dependent inhibitor effects for all measured analytes** (related to Supplementary Fig. 8, which includes only the 6CK set).

**Supplementary Figure 11 Confidence weights of  $\beta$  coefficients for all measured analytes** (related to Supplementary Fig. 9, which includes only the 6CK set).

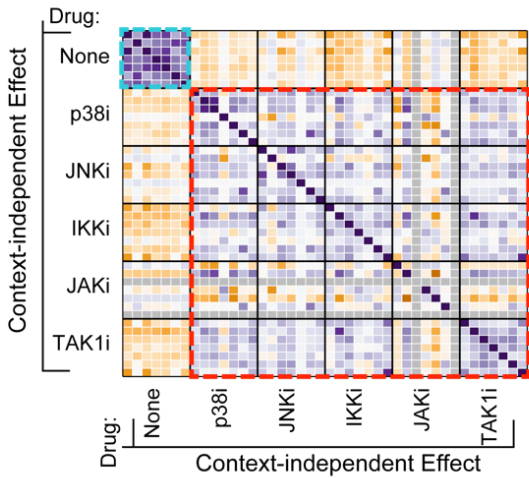
# Supplemental Figure 12



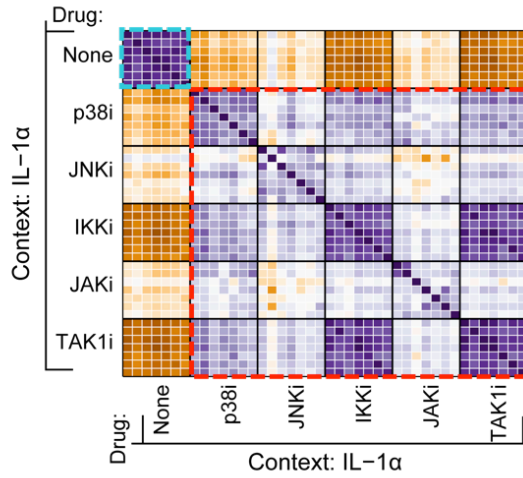
**Supplementary Figure 12  $\beta$  coefficients compiled across all SF samples and all stimulatory contexts.** (a) Trace plot showing relative magnitude of  $\beta$  coefficients averaged across all donor samples for basal conditions (“nostim”) or TNF $\alpha$ , IL-1 $\alpha$ , or Poly(I:C) stimulation for all measured analytes. (b) Heatmap of  $\beta$  coefficients compiled across all SF samples and stimulatory contexts (rows) for each of the measured cytokines and proteases (columns); coefficients have been scaled according to the maximum absolute value for each column.

# Supplemental Figure 13

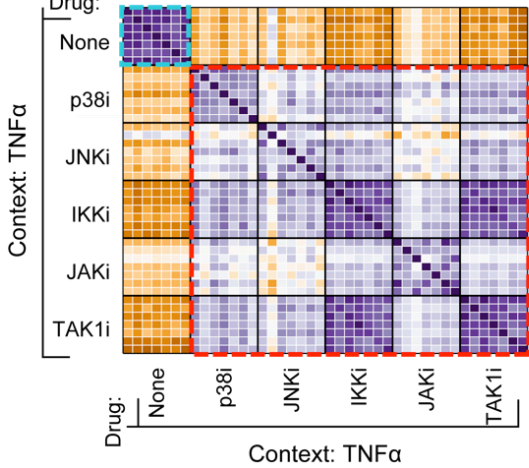
**a** Correlation between  $\beta$  coefficients



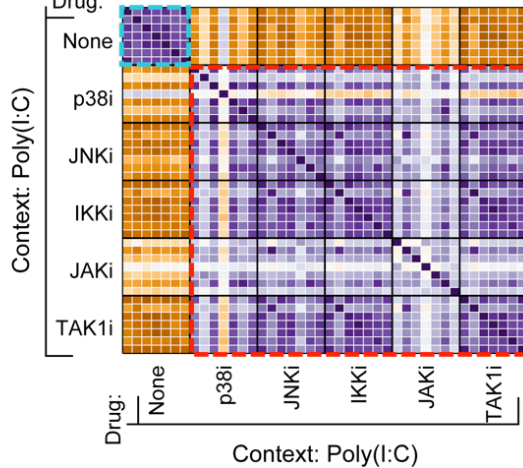
**b**



**c**



**d**



**Key to samples**

1.	N2586
2.	N2645
3.	N2759
4.	RA1869
5.	RA1931
6.	RA2159
7.	RA2708

1 2 3 4 5 6 7

---

**Key to drugs**

p38i: PH-797804  
 JNKi: JNK-IN-8  
 IKKi: IKK 16  
 JAKi: Tofacitinib  
 TAK1i: (5z)-7-oxozeaenol

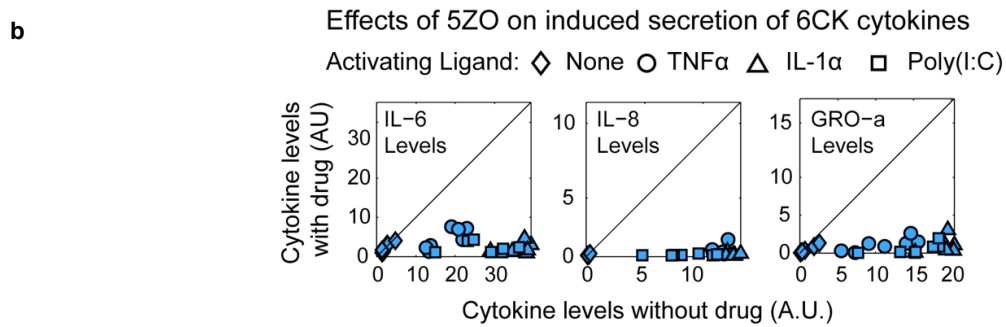
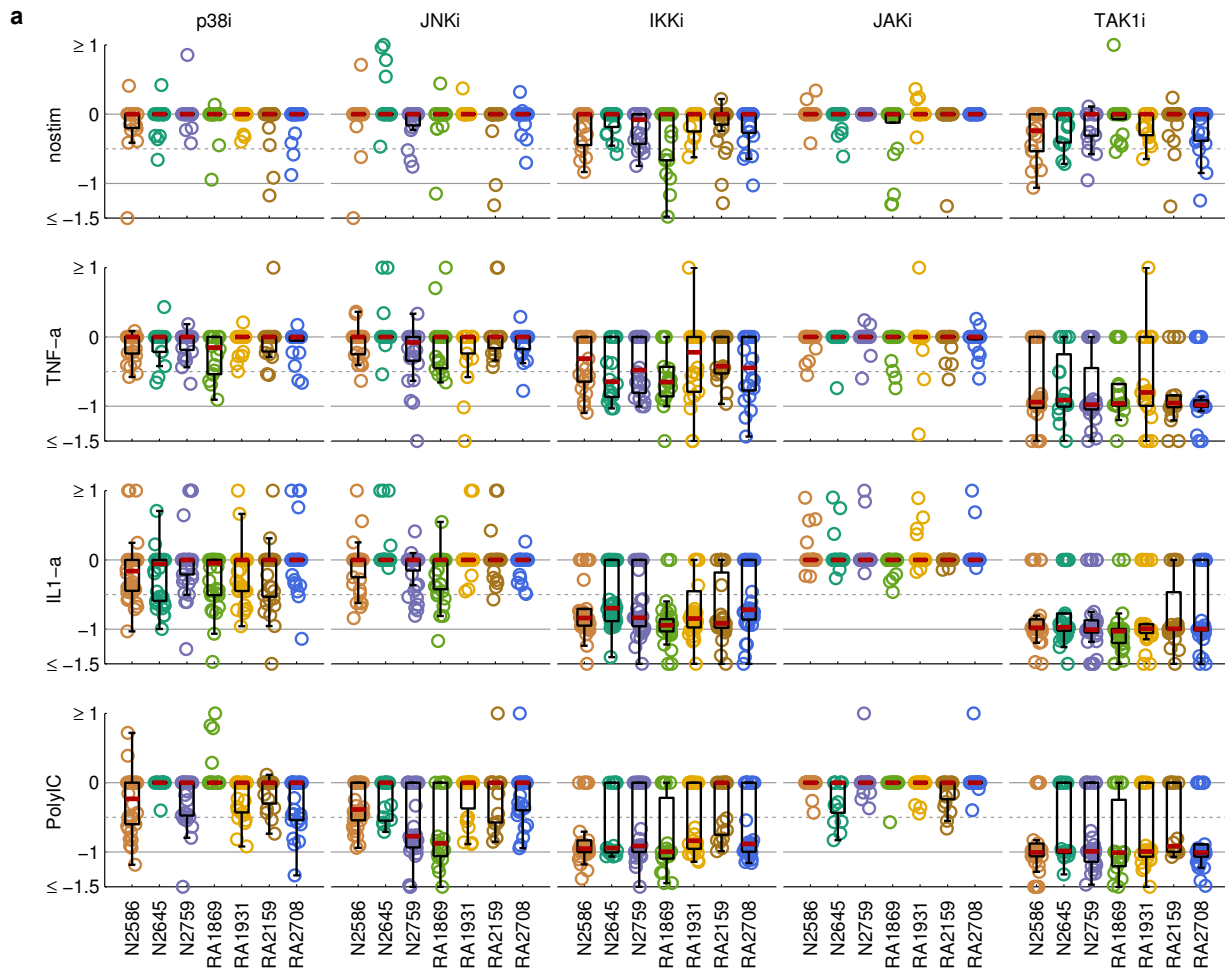
---

**Spearman coefficient**

1  
0.8  
0.6  
0.4  
0.2  
0  
-0.2  
-0.4  
-0.6  
-0.8  
-1

**Supplementary Figure 13 Spearman correlation of  $\beta$  coefficients across activating ligands, drugs and donor samples** (related to Figure 4b; panel **c** is reproduced from Fig. 4c for comparison). Correlation between  $\beta$  coefficients across the full cytokine/protease profile for context-independent (**a**) or context-dependent (**b-d**) effects. Heavy black gridlines distinguish  $7 \times 7$  matrices for the seven SF donor samples shown in the figure key. The light blue boxes designate the correlation of basal or stimulated secretion across the seven SF samples, and the red boxes designate the correlation between drug effects.

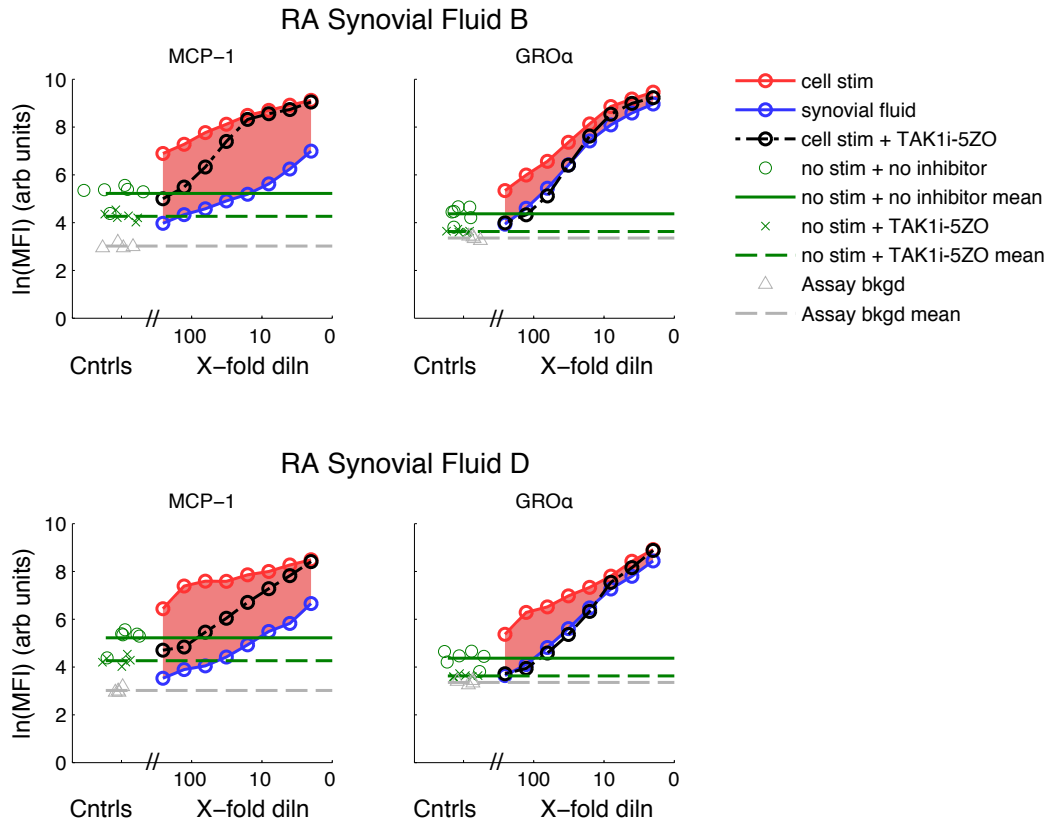
# Supplemental Figure 14



**Supplementary Figure 14** *Magnitude and direction of all inhibitor effects across donor samples and activating ligands* (related to Fig. 5a). **(a)** Distribution of  $\beta$  coefficients for inhibitors in Dataset 3 across the activated cytokines profiles with values scaled so that  $-1$  represents complete normalization to basal conditions and  $0$  represents no drug effect for the given context. Red dashes represents the median value of the distribution, boxes denote 25<sup>th</sup> and 75<sup>th</sup> percentile and whiskers represent  $\pm 2.7$  S.D. from the mean. In cases where boxes or whiskers are not shown, these values are overlapped by the median. p38i: PH-797804; JNKi: JNK-IN-8; IKKi: IKK 16; JAKi: tofacitinib; and TAK1i: 5ZO. **(b)** Raw data for selected 6CK cytokines IL-6, IL-8, and GRO I showing complete inhibition by 5ZO.

# Supplemental Figure 15

## 5ZO inhibits secretion induced by RA synovial fluids

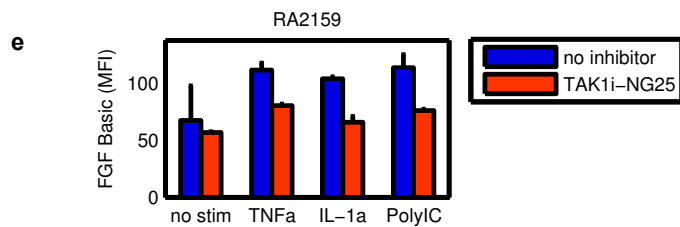
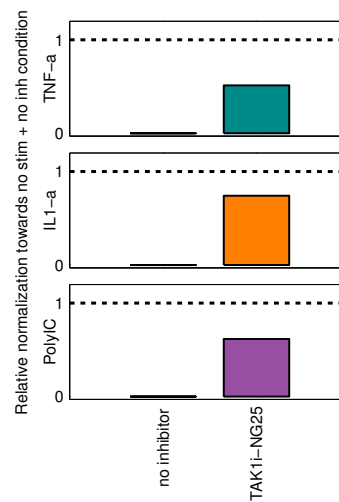
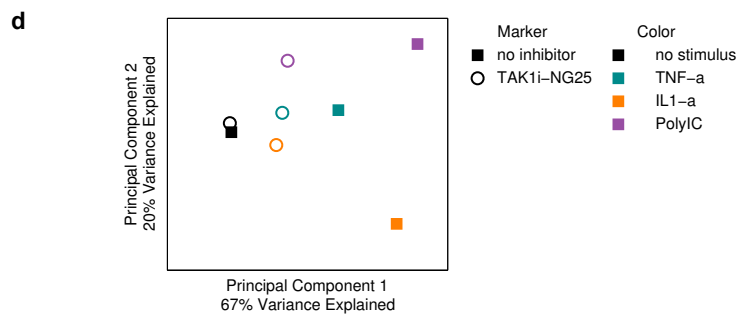
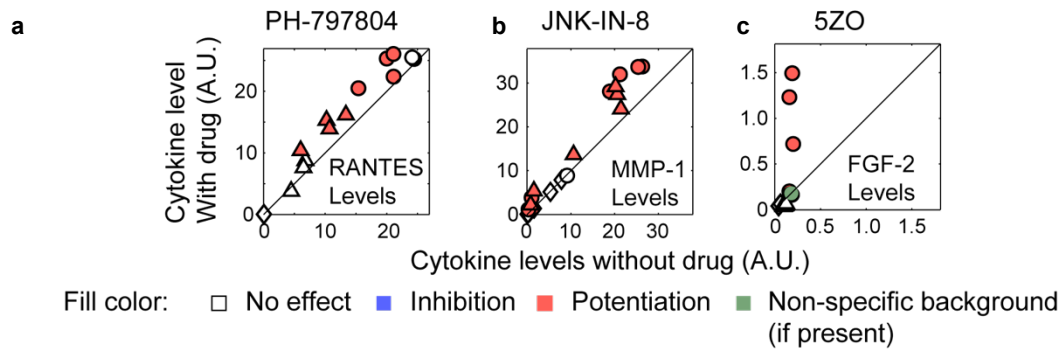


**Supplementary Figure 15** *5ZO inhibits the SF secretion response induced by RA synovial fluids* (related to Fig. 5d). Eight-point serial dilutions showing secretion response of MCP-1 and GRO $\alpha$  for RA synovial fluid samples B and D. 5ZO inhibits secretion of MCP-1 and GRO $\alpha$  induced by both donor samples. Red shaded regions corresponds amount of MCP-1 or GRO $\alpha$  attributable to secretion by SF.

# Supplemental Figure 16

## Potential counter-therapeutic drug effects

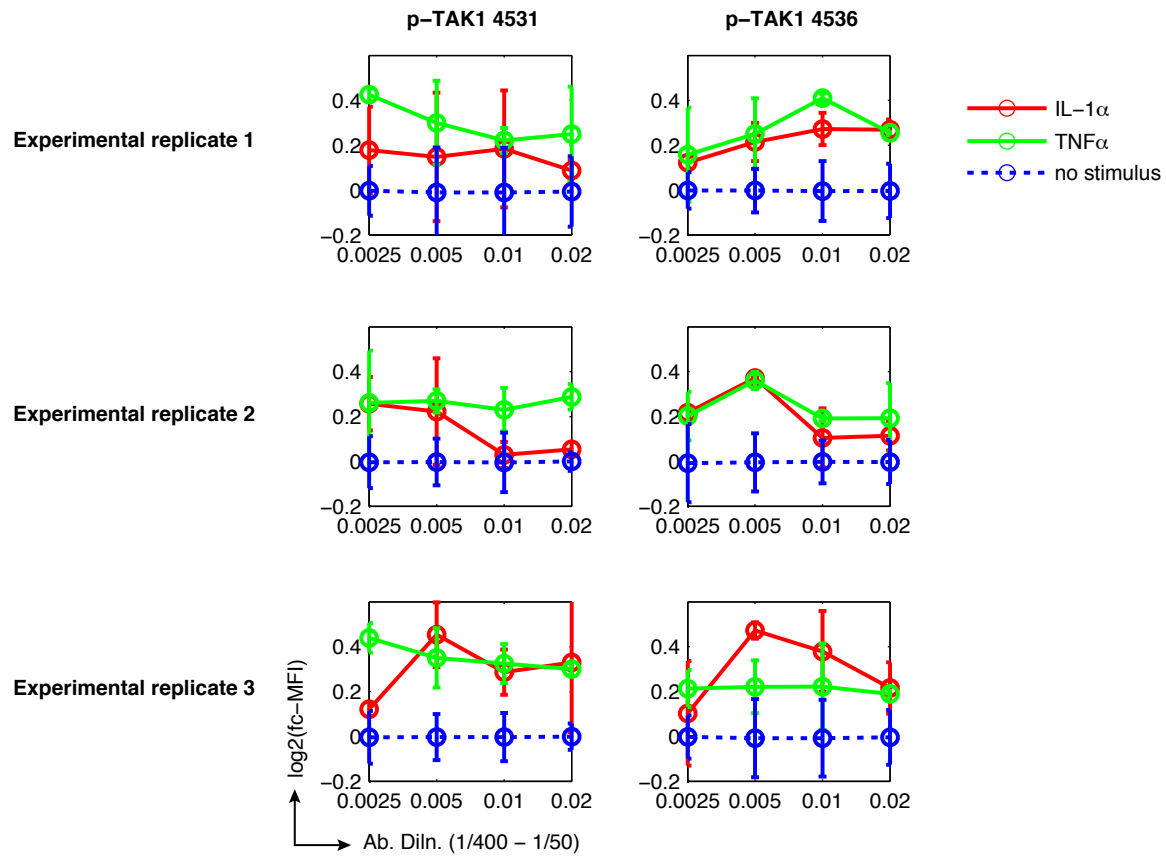
Activating Ligand:  $\diamond$  None  $\circ$  TNF $\alpha$   $\triangle$  IL-1 $\alpha$



**Supplementary Figure 16 *iMLR identifies potential counter-therapeutic effects.* (a-c)**

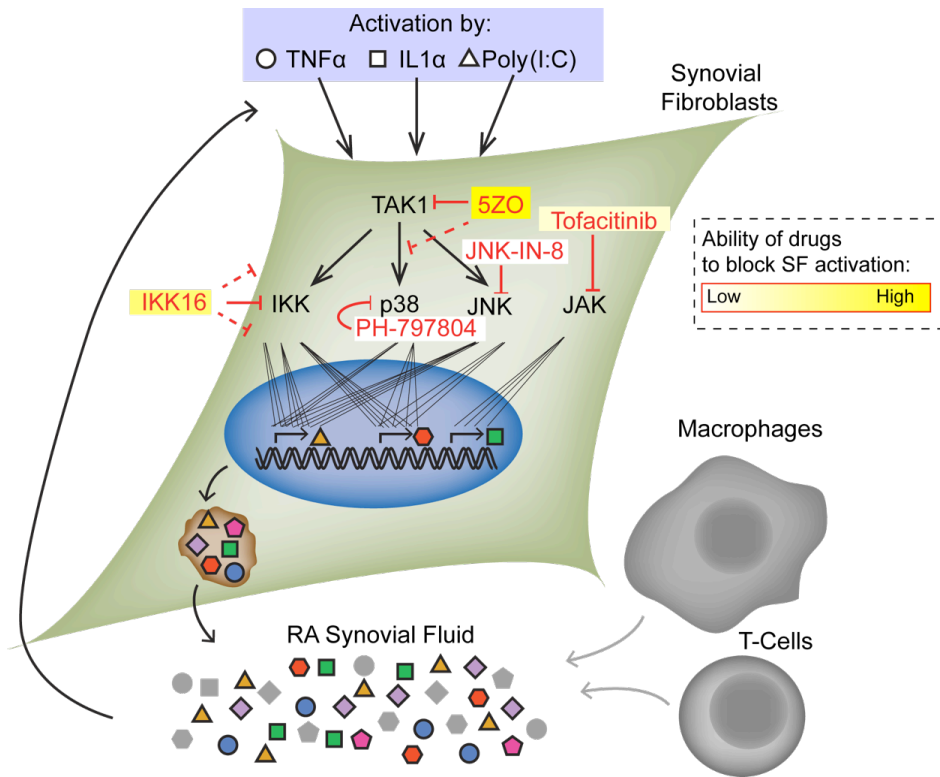
Undesirable effects of PH-797804, JNK-IN-8 and 5ZO were identified by iMLR; data points are colored to denote the directionality of kinase inhibitor effects as inferred by iMLR. A.U.: arbitrary units ( $10^3$  MFI units); weak cross-reactivity of TNF $\alpha$  to the FGF-2 detection antibody is shown in green, no other cross-reactivity by TNF $\alpha$  or IL-1 $\alpha$  against RANTES, MMP-1, or FGF-2 was detected. **(d-e)** Effects of TAK1i inhibitor NG25 on the activated SF cytokine profile. NG25 normalized activation of SF cytokine secretion induced by TNF $\alpha$ , IL-1 $\alpha$ , and Poly(I:C), panel **d**. NG25 displays lower potency than 5ZO, but it had to be used below its IC90 due to toxicity concerns at concentrations above 3  $\mu$ M (see Supplementary Figure 18). 3  $\mu$ M NG25 does not potentiate TNF $\alpha$ -induced FGF basic (FGF-2) secretion, panel **e**.

# Supplemental Figure 17



**Supplementary Figure 17 Phosphorylation of TAK1 by TNF $\alpha$  and IL-1 $\alpha$**  (related to Fig. 6a). SF were stimulated in biological duplicate with 100 ng/mL TNF $\alpha$  or IL-1 $\alpha$  for 10 min in the presence of 50 nM calyculin, a protein phosphatase 1a and 2 inhibitor (unstimulated condition was performed in quadruplicate). Cells were then fixed and stained with two phosphospecific TAK1 antibodies at a range of dilutions. Antibodies are denoted according to their Cell Signaling Technology cat. nos.: 4531 (p-TAK1 Thr184/187) and 4536 (p-TAK1 Thr187). Experiment was repeated on three separate days (total of 48 replicates for each stimulus and 96 replicates for no stimulus). These antibody dilutions and experimental replicates were averaged to produce the bar graph in Fig. 6a. fc-MFI: fold-change MFI relative to 'no stimulus'.

# Supplemental Figure 18



**Supplementary Figure 18 Schematic of SF activation by TNF $\alpha$ , IL-1 $\alpha$ , and Poly(I:C).**

Activation of SF results in secretion of inflammatory cytokines that contribute to the composition of synovial fluid and can also act in an autocrine manner. Other cell types, including immune cells, generate additional cytokines shown in gray. Inhibitors used in this study are associated with their primary targets, though the IKK inhibitor IKK 16 does display polypharmacology.

**Supplementary Data Legends**

**Supplementary Data 1-7 Raw data and iMLR X matrices for each SF sample.** Raw primary MFI data (spreadsheets: Ymat\_rep1 and Ymat\_rep2), Luminex bead counts (spreadsheets: YmatLMXbeadcount\_rep1 and YmatLMXbeadcount\_rep2), and iMLR independent variables (spreadsheets: Xmat\_rep1 and Xmat\_rep2) for the two experimental replicates (performed on separate days) and seven SF donor samples. Rows are individual experimental conditions and columns are Luminex data for individual cytokine analytes.

**Supplementary Data 1:** SF donor sample N2586

**Supplementary Data 2:** SF donor sample N2645

**Supplementary Data 3:** SF donor sample N2759

**Supplementary Data 4:** SF donor sample RA1869

**Supplementary Data 5:** SF donor sample RA1931

**Supplementary Data 6:** SF donor sample RA2159

**Supplementary Data 7:** SF donor sample RA2708

**Supplementary Data 8-14  $\beta$  coefficients and model stats.** iMLR  $\beta$  coefficients and model statistics. Beta coefficients (averaged across individual multimodeling solution algorithms) for individual experimental replicates (spreadsheets: Beta\_multimodAvg\_rep1 and Beta\_multimodAvg\_rep2), confidence weights (spreadsheets: ConfWt\_rep1 and ConfWt\_rep2), model statistics (spreadsheets: Stats\_rep1 and Stats\_rep2), and  $\beta$  coefficients and confidence weights merged across the two experimental replicates (spreadsheets: beta\_MergeReps and ConfWt\_MergeReps). For  $\beta$  coefficients and confidence weights spreadsheets, columns comprise beta coefficients for models of individual cytokines and rows specify global stimulus

(stimulus with no inhibitor), global inhibitor (inhibitor with no stimulus), and context-dependent inhibitor effects (inhibitor on the background of a given stimulus). Coefficients for cross-reactivity of stimuli against Luminex analytes are also included (rows for TNF-a\_L, IL1-a\_L, and PolyIC\_L).

**Supplementary Data 8:** SF donor sample N2586

**Supplementary Data 9:** SF donor sample N2645

**Supplementary Data 10:** SF donor sample N2759

**Supplementary Data 11:** SF donor sample RA1869

**Supplementary Data 12:** SF donor sample RA1931

**Supplementary Data 13:** SF donor sample RA2159

**Supplementary Data 14:** SF donor sample RA2708

### Supplementary Materials References

1. Taylor, P. C. & Feldmann, M. Anti-TNF biologic agents: still the therapy of choice for rheumatoid arthritis. *Nat Rev Rheumatol* **5**, 578–582 (2009).
2. Gibbons, L. J. & Hyrich, K. L. Biologic Therapy for Rheumatoid Arthritis. *BioDrugs* **23**, 111–124 (2009).
3. Hwang, S. Y., Kim, J. Y., Kim, K. W., Park, M. K. & Moon, Y. IL-17 induces production of IL-6 and IL-8 in rheumatoid arthritis synovial fibroblasts via NF-kappaB-and PI3-kinase/Akt-dependent pathways. *Arthritis Research & Therapy* **6**, R120–R128 (2004).
4. Tilg, H. & Moschen, A. R. Adipocytokines: mediators linking adipose tissue, inflammation and immunity. *Nat Rev Immunol* **6**, 772–783 (2006).
5. Neumann, E., Frommer, K. W., Vasile, M. & Müller-Ladner, U. Adipocytokines as driving forces in rheumatoid arthritis and related inflammatory diseases? *Arthritis & Rheumatism* **63**, 1159–1169 (2011).
6. Nah, S.-S. *et al.* Epidermal growth factor increases prostaglandin E2 production via ERK1/2 MAPK and NF-κB pathway in fibroblast like synoviocytes from patients with rheumatoid arthritis. *Rheumatol Int* **30**, 443–449 (2009).
7. Tavera, C. *et al.* IGF and IGF-binding protein system in the synovial fluid of osteoarthritic and rheumatoid arthritic patients. *Osteoarthritis and Cartilage* **4**, 263–274 (1996).
8. Boström, E. A. *et al.* Resistin and insulin/insulin-like growth factor signaling in rheumatoid arthritis. *Arthritis & Rheumatism* **63**, 2894–2904 (2011).
9. Hennessy, E. J., Parker, A. E. & O'Neill, L. A. J. Targeting Toll-like receptors: emerging therapeutics? *Nat Rev Drug Discov* **9**, 293–307 (2010).
10. Scheller, J., Chalaris, A., Schmidt-Arras, D. & Rose-John, S. The pro- and anti-inflammatory properties of the cytokine interleukin-6. *Biochimica Biophysica Acta - Mol Cell R* **1813**, 878–888 (2011).
11. Baggiolini, M. & Clark-Lewis, I. Interleukin-8, a chemotactic and inflammatory cytokine. *FEBS Lett.* **307**, 97–101 (1992).
12. Moser, B., Clark-Lewis, I., Zwahlen, R. & Baggiolini, M. Neutrophil-activating properties of the melanoma growth-stimulatory activity. *J. Exp. Med.* **171**, 1797–1802 (1990).

13. Schumacher, C., Clark-Lewis, I., Baggiolini, M. & Moser, B. High- and low-affinity binding of GRO alpha and neutrophil-activating peptide 2 to interleukin 8 receptors on human neutrophils. *Proceedings of the National Academy of Sciences* **89**, 10542–10546 (1992).
14. Carr, M. W., Roth, S. J., Luther, E., Rose, S. S. & Springer, T. A. Monocyte chemoattractant protein 1 acts as a T-lymphocyte chemoattractant. *Proceedings of the National Academy of Sciences* **91**, 3652–3656 (1994).
15. Xu, L. L., Warren, M. K., Rose, W. L., Gong, W. & Wang, J. M. Human recombinant monocyte chemotactic protein and other C-C chemokines bind and induce directional migration of dendritic cells in vitro. *Journal of Leukocyte Biology* **60**, 365–371 (1996).
16. Maghazachi, A. A., Al-Aoukaty, A. & Schall, T. J. CC chemokines induce the generation of killer cells from CD56+ cells. *Eur. J. Immunol.* **26**, 315–319 (1996).
17. Conti, P. & DiGiacchino, M. MCP-1 and RANTES are mediators of acute and chronic inflammation. *Allergy Asthma Proc* **22**, 133–137 (2001).
18. Taub, D. D. *et al.* Recombinant human interferon-inducible protein 10 is a chemoattractant for human monocytes and T lymphocytes and promotes T cell adhesion to endothelial cells. *J. Exp. Med.* **177**, 1809–1814 (1993).
19. Davies, S. P., Reddy, H., Caivano, M. & Cohen, P. Specificity and mechanism of action of some commonly used protein kinase inhibitors. *Biochem. J.* **351**, 95–105 (2000).
20. Davis, M. I. *et al.* Comprehensive analysis of kinase inhibitor selectivity. *Nature Biotechnology* **29**, 1046–1051 (2011).
21. Barrett, S. D. *et al.* The discovery of the benzhydroxamate MEK inhibitors CI-1040 and PD 0325901. *Bioorganic & Medicinal Chemistry Letters* **18**, 6501–6504 (2008).
22. Folkes, A. J. *et al.* The Identification of 2-(1H-Indazol-4-yl)-6-(4-methanesulfonyl-piperazin-1-ylmethyl)-4-morpholin-4-yl-thieno[3,2-d]pyrimidine (GDC-0941) as a Potent, Selective, Orally Bioavailable Inhibitor of Class I PI3 Kinase for the Treatment of Cancer. *J. Med. Chem.* **51**, 5522–5532 (2008).
23. Yan, L. MK-2206: a potent oral allosteric AKT inhibitor. *Proc Am Assoc Cancer Res Abstract No. DDT01–1* (2009).
24. Selness, S. R. *et al.* Discovery of PH-797804, a highly selective and potent inhibitor of p38 MAP kinase. *Bioorganic & Medicinal Chemistry Letters* **21**, 4066–4071 (2011).
25. Changelian, P. S. *et al.* Prevention of organ allograft rejection by a specific Janus kinase 3 inhibitor. *Science* **302**, 875–878 (2003).
26. Quintás-Cardama, A. *et al.* Preclinical characterization of the selective JAK1/2 inhibitor INCB018424: therapeutic implications for the treatment of myeloproliferative neoplasms. *Blood* **115**, 3109–3117 (2010).
27. Hexner, E. O. *et al.* Lestaurtinib (CEP701) is a JAK2 inhibitor that suppresses JAK2/STAT5 signaling and the proliferation of primary erythroid cells from patients with myeloproliferative disorders. *Blood* **111**, 5663–5671 (2008).
28. Weisel, K. C., Yildirim, S., Schweikle, E., Kanz, L. & Möhle, R. Effect of FLT3 inhibition on normal hematopoietic progenitor cells. *Ann. N. Y. Acad. Sci.* **1106**, 190–196 (2007).
29. Miknyoczki, S. J., Dionne, C. A., Klein-Szanto, A. J. & Ruggeri, B. A. The novel Trk receptor tyrosine kinase inhibitor CEP-701 (KT-5555) exhibits antitumor efficacy against human pancreatic carcinoma (Panc1) xenograft growth and in vivo invasiveness. *Ann. N. Y. Acad. Sci.* **880**, 252–262 (1999).
30. Zhang, T. *et al.* Discovery of potent and selective covalent inhibitors of JNK. *Chemistry & Biology* **19**, 140–154 (2012).

31. Waelchli, R. *et al.* Design and preparation of 2-benzamido-pyrimidines as inhibitors of IKK. *Bioorganic & Medicinal Chemistry Letters* **16**, 108–112 (2006).
32. International Centre for Kinase Profiling. Accessed Feb 2015 at <<http://www.kinase-screen.mrc.ac.uk/screening-compounds/349381>>
33. Tan, L. *et al.* Discovery of Type II Inhibitors of TGF $\beta$ -Activated Kinase 1 (TAK1) and Mitogen-Activated Protein Kinase Kinase Kinase 2 (MAP4K2). *J. Med. Chem.* **58**, 183–196 (2015).
34. Benjamini, Y. & Hochberg, Y. Controlling the false discovery rate: a practical and powerful approach to multiple testing. *Journal of the Royal Statistical Society Series B* (1995). doi:10.2307/2346101